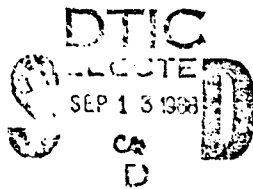MRL-R-1117

AR-005-231

AD-A198 986

DEPARTMENT OF DEFENCE

DEFENCE SCIENCE AND TECHNOLOGY ORGANISATION

MATERIALS RESEARCH LABORATORY

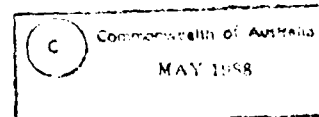#### MELBOURNE, VICTORIA

REPORT

MRL-R-1117

AN ANALYSIS OF AN IMPLICIT FACTORED SCHEME
FOR SIMULATING SHOCK WAVES

DTIC
ELECTE
SEP 1 3 1988
Ca
D

M.B Tyndall

Approved for Public Release

DSTO
MELBOURNE

(C) Commonwealth of Australia
MAY 1988

88 9 13 046

DEPARTMENT OF DEFENCE

MATERIALS RESEARCH LABORATORY

REPORT

MRL-R-1117

AN ANALYSIS OF AN IMPLICIT FACTORED SCHEME
FOR SIMULATING SHOCK WAVES

M.B. Tyndall

ABSTRACT

A detailed derivation and analysis of an implicit factored scheme (Beam and Warming 1976) is given. A one dimensional shock tube problem is solved numerically using the factored scheme. The results and exact solution are presented for this problem. An analysis of the features of the method is made and the limitations of this implicit factored scheme for more general applications to shock waves in solids are discussed. An alternative approach which has been developed by Boris and Book (1976) appears to have wider applicability than the method studied here.

Approved for Public Release

CONTENTS

2

TABLE OF SYMBOLS

A	the Jacobian matrix of the flux vector $\mathbf{F}$
c	the local speed of sound
E	total energy per unit volume
E_i	total energy per unit volume in region i
$F(U)$	the flux vector for the conservative form of the one-dimensional Euler equations
i	subscript denoting the regions in the exact solution of the Riemann problem
I	the identity matrix
j	subscript denoting the grid points in the x-direction
k	subscript denoting the eigenvalues of A
L	matrix operators
n	superscript denoting time index
p	the pressure
p_i	the pressure in region i
Q	matrix of eigenvectors of A
t	time
u	the particle velocity
u_i	the particle velocity in region i
U	the shock velocity
$\mathbf{U}$	the flow vector for the conservative form of the one-dimensional Euler equation
x	the space variable
x_i	the region boundaries
α_m	constant used in finite difference expressions ($m=1,2,3$)
γ	the ratio of specific heats
δ_x^b	a backward difference operator
δ_x^f	a forward difference operator
Δt	the time increment
Δx	the space increment
Δ_x	the classical forward difference operator
ϵ	total energy per unit mass
θ	parameter related to the choice of time differencing
λ_k	eigenvalues of the Jacobian matrix A
Λ	the diagonal matrix of the eigenvalues λ_k
ξ	parameter related to the choice of time differencing
ρ	the density
ρ_i	the density in region i
∇_x	the classical backward difference operator

3

1. INTRODUCTION

In this report a detailed analysis of an implicit finite-difference algorithm (Beam and Warming 1976) for solving nonlinear hyperbolic systems in conservative form is given. This method is one of many finite-difference schemes used to solve systems of hyperbolic equations. Familiar schemes for solving these systems include the finite-difference methods of Godunov, Lax and Wendroff, McCormack, the upwind scheme, the hybrid scheme of Harten and Zwas, and the flux corrected transport (FCT) method of Boris and Book. An excellent review of these methods and others is given by Sod 1978. The cubic-interpolated pseudo particle (CIP) method (Takewaki and Yabe 1987) and finite element flux corrected transport (Lohner and others 1987) are just two of the more recent methods in use. All of these methods are most commonly used to solve the Euler and Navier-Stokes equations. This report looks at a one-dimensional shock tube problem using the Eulerian (inviscid) gasdynamic equations.

This analysis was prompted by the need to find a suitable numerical method that could efficiently and accurately model shock waves in two-dimensional solids. Beam and Warming 1976 presented and solved problems involving shock waves in two-dimensional inviscid gases, such as transonic aerodynamics and shock boundary-layer interactions. For this report a one-dimensional form of the algorithm given in Beam and Warming 1976 was used to model shock waves in an inviscid gas. Based on the performance in this problem this numerical method was assessed for its suitability to model the more difficult problem of shocks in two-dimensional solids, where the solids are assumed to behave hydrodynamically.

There are numerous difficulties that are encountered when trying to model shock waves numerically. Some are related to the specific problem, eg. steep gradients and boundary conditions, others to the numerical method that is being used, eg. damping, dispersion and non-physical oscillations (Gibbs error) while others effect the whole system eg. accuracy and stability. The main aim of choosing a particular numerical method is that it must minimize these difficulties. In choosing a suitable finite-difference algorithm there is a set of basic requirements to be satisfied. A complete list is given by Boris and Book 1976b. The requirements of most importance are:

1. Exact conservation properties of the physical equations should be mirrored in the numerical method used.

2. The numerical method must be stable for a range of grid spacings and time steps.

3. The density ρ should remain positive.

4

4. The numerical method should provide at least second order accuracy in *regions of the problem*, eg. the shock front.

5. The numerical method should be fast and efficient.

These requirements are listed in order of decreasing importance. The first three requirements must be satisfied by the finite-difference algorithm otherwise the results cannot be considered to be realistic. As well as these requirements the more difficult problems will require a finite-difference algorithm that is fairly robust and can cope with a wide range of boundary conditions and equations of state. For modelling of shock waves in solids, elastic-plastic terms must also be included and tolerated by the algorithm.

An implicit finite difference scheme has been chosen here to solve the one-dimensional form of the inviscid gasdynamic equations. Long computational times have excluded the possibility of using an explicit finite difference scheme since the stability bound of an explicit algorithm forces a time step that can be orders of magnitude smaller than that required for accuracy. There is a limited number of spatial difference approximations that can be used for the conservative form of the inviscid gasdynamic equations. Only centered difference operators lead to difference methods that are simultaneously stable for both positive and negative characteristic speeds (i.e. eigenvalues) that are associated with spatial flux terms. One-sided (or upwind) schemes can be used when the flux terms are split into components corresponding to either their negative or positive characteristic speeds. One-sided schemes have superior dissipative and dispersive properties compared to those of centered schemes (Steger and Warming 1981). Therefore a more robust and efficient algorithm can be obtained by splitting the flux terms and applying one-sided differences. The implicit factored scheme developed by Beam and Warming 1976 incorporates these principles and is the more commonly used method of this type.

In the second section a brief description of the implicit factored scheme of Beam and Warming 1976 is given. The Riemann problem in one dimension is solved numerically with this method. A discussion of this problem is given in Section 3 and the results are presented in the Section 4. Section 5 sums up the analysis and compares this method with others and conclusions are drawn concerning the suitability of the Beam and Warming algorithm for modelling shock waves in solids.

2. AN IMPLICIT FACTORED SCHEME

In this section a brief summary of the one-dimensional form of the method in Beam and Warming 1976 is given. A full derivation is presented in Appendix A.

2.1 One Dimension

In one dimension the Eulerian inviscid gasdynamic equations (Appendix A), namely the continuity equation, conservation of mass and conservation of energy, c. be written in conservation (or vector) form as

$$\frac{\partial U}{\partial t} + \frac{\partial F(U)}{\partial x} = 0 \tag{1}$$

where

$$U = \begin{pmatrix} \rho \\ \rho u \\ E \end{pmatrix} \qquad F(U) = \begin{pmatrix} \rho u \\ \rho u^2 + p \\ (E+p)u \end{pmatrix} \tag{2}$$

ρ is the density, u the particle velocity, E the total energy per unit volume and the pressure $p = (\gamma - 1)[E - \frac{1}{2}\rho u^2]$, γ is the ratio of specific heats. An ideal gas equation of state is assumed.

Equation (1) is the fundamental system to solve. It is a form of the Euler equation for non-viscous fluids. The scheme divised by Beam and Warming 1976 uses a factorisation of the equation after time differencing. This approach relies on the explicit form of equation (1) including the use of an equation of state that can be expressed in the functional form

$$p = \rho f(\epsilon) \tag{3}$$

where ϵ is the internal energy per unit mass and f is a function. When the equation of state can be expressed in this functional form then the nonlinear flux vector $F(U)$ is a homogeneous function of degree one. Using this homogeneity property

$$F(U) = A(U)U \tag{4}$$

of the Euler equations, where A is the Jacobian matrix of F, a linear time-differenced form of equation (1) can be written (Appendix A) as

$$\left[I + \frac{\theta \Delta t}{1+\zeta}\frac{\partial}{\partial x}A^n\right]\Delta U^n = -\frac{\Delta t}{1+\zeta}\left(\frac{\partial F}{\partial x}\right)^n + \frac{\zeta}{1+\zeta}\Delta U^{n-1} + O[(\theta - \frac{1}{2} - \zeta)\Delta t^2 + \Delta t^3] \tag{5}$$

6

where I is the identity matrix, $\Delta U^n = U^{n+1} - U^n$, Δt the discrete time increment and $U(t) = U(n\Delta t) = U^n$. The parameters θ and ξ define the particular time-difference approximation that can be used. Examples of some familiar implicit schemes are

$$\theta = \frac{1}{2}, \qquad \xi = 0 \qquad \text{trapezoidal formula;}$$

$$\theta = 1, \qquad \xi = 0 \qquad \text{backward Euler;}$$

$$\theta = 1, \qquad \xi = \frac{1}{2} \qquad \text{three-point backward.}$$

The Jacobian matrix A has the eigenvalues u and $u \pm c$ where $c = \left(\frac{\gamma p}{\rho}\right)^{\frac{1}{2}}$ is the local speed of sound. One-sided spatial differences have superior properties when compared to centered spatial differences (Section 1). For this reason Beam and Warming 1976 use one-sided differences in their scheme. To be able to apply these one-sided spatial differences the flux terms must be split according to the sign of their characteristic speeds (i.e. eigenvalues). The flux-vector F can be split into two parts, F^+ and F^-, (see Appendix A) F^+ corresponds to the positive eigenvalues of A and F^- to the negative eigenvalues of A. The partial derivative $\frac{\partial}{\partial x}$ in equation (5) can be replaced with one-sided spatial difference approximations. To maintain the stability of the system a backward difference operator is used for positive eigenvalues of A and a forward difference operator for negative eigenvalues of A. By dropping the third order term $O(\Delta t^3)$, splitting the flux vectors and applying one-sided spatial differences to equation (5), a noniterative implicit finite-difference scheme for equation (1), that is second order accurate, can be written as,

$$\left(1 + \frac{\theta \Delta t}{\Delta x(1+\xi)}\nabla_x A_j^+|^n\right)\Delta U_j^* = -\frac{\Delta t}{2\Delta x(1+\xi)}\left(\delta_x^b F_j^+|^n + \delta_x^f F_j^-|^n\right) + \frac{\xi}{1+\xi}\Delta U_j^{n-1} \quad (6a)$$

$$\left(I + \frac{\theta \Delta t}{\Delta x(1+\xi)}\Delta_x A_j^-|^n\right)\Delta U_j^n = \Delta U_j^* \quad (6b)$$

$$U_j^{n+1} = U_j^n + \Delta U_j^n \quad (6c)$$

where $x = j\Delta x$, ∇_x is the classical backward difference operator defined in Appendix A (equation (A26)) and Δ_x the classical forward difference operator defined in Appendix A (equation (A27)); δ_x^b and δ_x^f defined in Appendix A (after equation (A28)). The flow vector U in equation (1) has been replaced by U_j^n, where the superscript n denotes the time level and the subscript j denotes the grid point location. The notation A_j^n means the value of A evaluated at time level n.

Equations (6) can be further simplified to

$$L_j^+|^n \Delta U_j^* = \alpha_1 A_{j-1}^+|^n \Delta U_{j-1}^* + \alpha_2\left(\delta_x^b F_j^+|^n + \delta_x^f F_j^-|^n\right) + \alpha_3 \Delta U_j^{n-1} \quad (7a)$$

$$L_j^-|^n \Delta U_j^n = \Delta U_j^* - \alpha_1 A_{j+1}^-|^n \Delta U_{j+1}^n \quad (7b)$$

7

$$U_j^{n+1} = U_j^n + \Delta U_j^n \tag{7c}$$

where

$$L_j^+|^n = I + \alpha_1 A_j^+|^n \tag{8}$$

$$L_j^-|^n = I - \alpha_1 A_j^-|^n \tag{9}$$

and

$$\alpha_1 = \frac{\theta \Delta t}{\Delta x(1+\xi)} \tag{10a}$$

$$\alpha_2 = \frac{\Delta t}{2\Delta x(1+\xi)} \tag{10b}$$

$$\alpha_3 = \frac{\xi}{1+\xi}. \tag{10c}$$

Equations (7) describe an algorithm that can be used to solve equation (1). To avoid large-amplitude oscillations, especially in shock wave solutions, a fourth-order dissipation term is added to the right hand side of equation (7a). A fourth-order dissipation term has been chosen so that the formal order of the scheme is not disrupted. The dissipation term is of the form

$$-(\omega/8)\Delta x^4(\partial^4 U/\partial x^4)|_j^n \approx -(\omega/8)(U_{j+2}^n - 4U_{j+1}^n + 6U_j^n - 4U_{j-1}^n + U_{j-2}^n) \tag{11}$$

The above scheme (equations (7) and (11)) is stable for values of ω in the range $0 \leq \omega \leq 1$ according to a linearised von Neumann stability analysis (Beam and Warming 1976). This implicit factored scheme is easy to implement when compared to an algorithm with centered spatial differences, which usually involve the inversion of tridiagonal and pentadiagonal matrices. This brief summary highlights the simplifications that can be made for nonlinear systems whose flux vectors are homogeneous functions (of degree one). The most important of these simplifications is the splitting of the flux vectors into subvectors which correspond to their characteristic speeds.

2.2 Two Dimensions

Beam and Warming 1976 also applied this implicit factored scheme to the two-dimensional Eulerian invisicid gasdynamic equations. The value of this approach may be seen from the large number of problems in the literature to which it has been applied. These include transonic aerodynamics, i.e. lifting and nonlifting of airfoils oscillating in a free stream (Beam and Warming 1976 and Steger and Warming 1981), Couette flow, shock boundary-layer interactions (Beam and Warming 1978) and in one-dimensional shock tube flow (Steger and Warming 1981), see Section 3.

8

Beam and Warming 1978 used the Couette flow problem (unsteady flow between two infinite adiabatic parallel walls) as a test problem for their two-dimensional algorithm. The spatial accuracy and stability of the numerical algorithm as well as its boundary conditions were chosen as the initial test. The numerical solution when compared to the analytical solution exhibited a good degree of accuracy. No numerical dissipation was added to the numerical algorithm for this problem. The shock boundary-layer problem was used as a more severe test for the two-dimensional algorithm. No analytical solution for this problem was available for comparison but when compared to the numerical solution obtained by other methods this method was in good agreement.

Steger and Warming 1981 developed new explicit and implicit dissipative finite-differences for the one-dimensional and two-dimensional forms of the inviscid gasdynamic equations. These different methods were used to solve the one-dimensional shock tube problem (see Section 3) and the two-dimensional problem of transonic airfoils. Centered spatial differences were also used and compared to upwind differences (used for the split flux formulation). The implicit upwind scheme (the method used in this report) solved the one-dimensional shock tube problem better than the other individual methods. Although the combined algorithm of an explicit upwind scheme and explicit MacCormack scheme (Steger and Warming 1981) was an improvement on the implicit upwind scheme. For the two-dimensional problem, the conventional implicit algorithm using centered differences was compared to the implicit upwind algorithm. The results obtained for the airfoil problem using these two different algorithms were in good agreement although there were small oscillations in the implicit upwind solution. These oscillations were due to the conservative flux vectors having discontinuous derivatives i.e. the eigenvalues changing sign. By adding blending terms to the eigenvalues (Steger and Warming 1981) the oscillations were smoothed out. Beam and Warming 1976 used a hybrid scheme with a fourth-order dissipative term (similar to (11)) to solve this airfoil problem. This solution agreed with that of Steger and Warming 1981 and had no oscillations.

3. A SIMPLE ONE-DIMENSIONAL PROBLEM

A stringent test for non-linear systems described by the equations (1) and (2) is the one-dimensional shock tube or Riemann problem. This is a simple problem where a diaphragm separates two regions of different pressures and densities. The fluid on each side of the diaphragm is an ideal gas which is at rest at time $t = 0$. The initial conditions for this problem are shown in Fig. 1(a). The diaphragm is placed at $x = 0$ and $\rho_1 > \rho_5$. The pressures are assumed to be such that $p_1 > p_5$.

Equations (1) and (2) can be solved exactly for this problem (Takewaki and Yabe 1987) enabling a precise assessment of the numerical method. This solution is presented in detail in Appendix B and illustrated in Figure 1(b) for density, 1(c) for pressure, 1(d) for total energy and 1(e) for particle velocity. Because of the step changes in physical properties, as shown in Figs 1, the Riemann problem is considered a severe test of the capability of numerical methods to solve the Euler equations. When the diaphragm is ruptured ($t > 0$, see Fig. 1(b)), an expansion propagates into the high-pressure gas and a shock wave followed by a contact discontinuity, propagates into the low-pressure gas. Region 2 in Fig 1(b) represents the area of adiabatic expansion, region 3 the contact discontinuity and region 4 the shock wave. A paricular numerical method's accuracy and performance can be determined when the exact solution and the numerical solution are compared, especially at the contact discontinuity and the shock front.

The Beam and Warming method was tested against this Riemann problem using equations (7) and three-point backward time-differencing ($\theta = 1$ and $\xi = \frac{1}{2}$). The three examples of implicit time-differencing given in Section 2, the trapezoidal formula, the backward Euler differencing and the three-point backward differencing, were all used to solve the Riemann problem. There were no significant differences between the solutions given by these different time-differencing schemes, except that the trapezoidal formula was unstable for $t > 0.001$. Hence only the three-point backward time-differencing was used for this section. The scheme is unconditionally stable for $\theta = 1$ and $\xi = \frac{1}{2}$ (Steger and Warming 1981).

The dissipation term given in equation (11), was added to the right hand side of equation (7a), with $\omega = 0.5$. One hundred points were taken each side of the diaphragm with $\Delta x = 0.025$, so that, x was in the range $-2.5 \leq x \leq 2.5$. The ratio of specific heats, γ, was 1.4 and the initial conditions were $\rho_1 = p_1 = 10.0$, $\rho_5 = p_5 = 1.0$ and $u_1 = u_5 = 0$.

There was a fixed boundary at $x = -2.5$ and at $x = 2.5$ i.e. $U_{N2}^n = U_{N2}^0$ and $U_{N1}^n = U_{N1}^0$ where n refers to the time step, 0 the initial time step, $N2$ the boundary $x = 2.5$ and $N1$ the boundary $x = -2.5$.

4. DISCUSSION OF RESULTS

Using the implicit factored scheme and the parameters given in Section 3, the Riemann problem was solved for different time increments ($\Delta t = 0.01$, $\Delta t = 0.005$, $\Delta t = 0.001$ and $\Delta t = 0.0001$) but for the same total time ($t = 1.0$). Each of the solutions Fig. 2-5 can be compared to the exact solution shown in Fig. 1(b)-1(e). The parameters and solution values for the exact solution are given in Table 1.

The density profile after 100 time steps ($\Delta t = 0.01$) is shown in Fig. 2(a). This profile follows the general form of the exact solution (Fig. 1(b)) except for a non-physical oscillation at the shock front $x = x_4$ and the smearing of the contact discontinuity and the shock front. Although both the contact surface and the shock front have both been smeared, this numerical scheme has resolved the shock front better i.e. there is less dispersion at $x = x_4$ than at $x = x_3$. By adding more dissipation (i.e. increasing the value of ω in equation (11)) the non-physical oscillation or the Gibbs type error effect can be reduced. To reduce the amplitude of the oscillation more dissipation was added in this way, but this was unsuccessful. The dissipation term is two orders of magnitude smaller than the overall scheme, hence by increasing ω there should be no significant changes in the solution as was observed. Recall from Section 2, the addition of a dissipation term should not effect the overall stability of the scheme and therefore has to be this small. Hence to improve the overall accuracy of the solution, which would also reduce the amplitude of the oscillation, the time step needs to be made smaller i.e. increase the number of time steps. Before considering a smaller time step it is worthwhile to look at this non-physical oscillation in the corresponding profiles of pressure, energy and velocity in Fig. 2(b), Fig. 2(c) and Fig. 2(d), respectively. Note that the oscillations occur at the sharp change in pressure, but not when the density changes with constant pressure. The oscillation is more pronounced in the pressure and energy profiles and is at its extreme in the velocity profile where it is producing negative velocities.

The time step has been reduced by a factor of a half ($\Delta t = 0.005$) in Fig. 3. The amplitude of the oscillation has been significantly reduced with only a small undershoot, consisting of three grid points, remaining. Also note that the boundaries $x = x_3$ and $x = x_4$ have not suffered any further dispersion. Reducing the time step again ($\Delta t = 0.001$), see Fig. 4, reduces the amplitude of the remaining undershoot at the shock front but the solution has become more diffuse with the contact surface and the shock front further dispersed. This has caused the solution to become less accurate when compared to the exact solution. This situation worsens when the time step is reduced again ($\Delta t = 0.0001$), see Fig. 5, where both the contact surface and the shock front have been severely dispersed. No oscillations occur, but compared to the exact solution in Fig. 1(b) the solution has become inaccurate. The best balance between the problems of non-physical oscillations and severe diffusion appears to be in Fig. 3 where $\Delta t = 0.005$. Obviously with different initial conditions and parameters a time step other than 0.005 would provide the required balance between diffusion and oscillations. The best value for Δt is a subjective compromise based on diffusion verses oscillations and can only be determined by trial and error

11

The Courant-Fredrichs-Lewy condition (CFL) was used to t   : stability of the scheme. The CFL condition for this particular hyperbolic scheme i<

$$|\lambda_k(U)|\frac{\Delta t}{\Delta x} \leq 1, \qquad k = 1, 2, 3. \tag{12}$$

where λ_k are the eigenvalues of the Jacobian matrix $A(U)$. Expressing this condition geometrically: the numerical domain of dependence of the scheme (7) (with equation (11) added) must contain the domain of dependence of the differential equation (Peyret and Taylor 1983) The solutions discussed above easily satisfied this condition. This is because the numerical scheme is unconditionally stable. The Courant number did become close to unity at $x = x_4$ (the shock front), however. This was the region where the oscillations occured, hence verifing that the oscillations were non-physical i.e. they were not part of the solution but an error of the scheme employed.

Ideally an infinite shock tube should be used for the one-dimensional shock tube problem and therefore any end boundary effects could be eliminated. This is not possible in practice since the numerical scheme that has been used here is an alternating direction (ADI) method (i.e equation (7a) is evaluated in the positive x direction and then equation (7b) is evaluated in the negative x direction). Therefore the boundaries at $x = -2.5$ and $x = 2.5$ are fixed. As can be seen from the results these boundaries are far enough away from the diaphragm, hence there is no boundary effect on the solution. With boundaries closer to the diaphragm the stability of the scheme and the numerical solution may have been adversely affected

The implicit factored scheme that has been employed here cannot be used when the flux-vector F is non-homogenorus. Recall that, if F satisfies the homogeneous property (refer to equation (4)) and A has a complete set of linearly independent eigenvectors then the flux vector F can be split into two subvectors, one subvector corresponding to the positive eigenvalues of A and the other the negative eigenvalues These subvectors can then be differenced individually with the appropriate one-sided scheme. If the flux vector is non-homogeneous then it cannot be split into subvectors and therefore an alternative algorithm using centered spatial differences has to be used. As noted in Section I algorithms using upwind differencing have superior dissipative and dispersive properties as well as being more robust and efficient than algorithms using centered differences. Therefore, to be able to solve an arbitrary nonlinear hyperbolic system (in conservation-law form) with this implicit factored scheme the equation of state, the nonlinear flux vectors must be homogeneous functions of degree one

5. CONCLUSIONS

Using the one-dimensional shock tube or Riemann problem, the implicit factored scheme developed by Beam and Warming 1976 has been tested for its capability to solve the Euler equations. The Riemann problem proved to be a severe test for this scheme. The scheme performed well but it had a couple of drawbacks. Non-physical oscillations (Gibbs error) and dispersion of the contact discontinuity and the shock front adversely affected the solution. By removing the oscillations the solution became more dispersed and by minimizing the dispersion the amplitude of the oscillations increased. Therefore the best solution for a problem (solved with this method) is a subjective compromise based on diffusion versus oscillations and can only be determined by trial and error. Besides these difficulties this implicit factored scheme was stable and efficient for a wide range of parameters.

The main motivation for this work was to examine a paricular numerical method to see if it could successfully model shock waves and be adapted for studying shocks in the solid state. After finding a suitable numerical method, the simple one-dimensional shock tube (Riemann) problem presented in Section 3 would be extended to model shock waves in solids, eg. the shock waves generated when a flyer-plate impacts a solid material. This requires different equations of state to the ideal gas equation used here. The ideal gas equation is a special case of the functional form of the equation of state (given in equation (2)), which this method is suitable for. If the equations of state for solids can be constructed in this functional form or if this functional form is used over restricted ranges of pressure and density then the implicit factored scheme can be used. If the equations of state for solids are not in this form then an alternative numerical scheme must be found. Elastic-plastic conditions must be incorporated into the problem and usually the addition of suitable source or sink terms to equation (1). Extensions to two dimensions and the possible incorporation of initiation and detonation of explosives would follow. These problems would obviously require a fairly robust and versatile numerical scheme. The implicit factored scheme used here performs well for the sample problem but the restrictions on the boundary conditions and the choices of equations of state are too restricive for our purposes.

Though not yet examined in detail by us other methods, such as flux-corrected transport (FCT) (Boris and Book 1973, Book, Boris and Hain 1975 and Boris and Book 1976a) and Zalesak 1979 multidimensional FCT appear to provide the accuracy and versatility ne ded for these problems. Results published elsewhere (Boris and Book 1973, Book, Boris and Hain 1975, Boris and Book 1976a, 1976b, Zalesak 1979, 1981 and Sod 1978) suggest that they are highly accurate and reasonably easy to use. An excellent example of this is in Zalesak 1981. The one-dimensional shock tube (Riemann) problem is solved using a FCT method with similar parameters to the problem solved here. The FCT method solves the shock tube problem extremely well. The solution is highly accurate and has superior results when compared to the method used here and other methods elsewhere (Sod 1978). Further investigations are taking place along these lines.
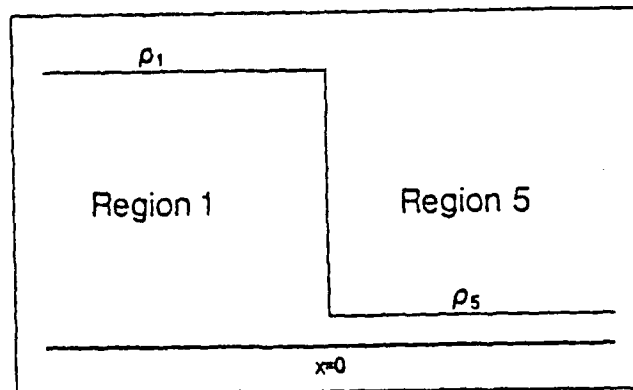
13

6. ACKNOWLEDGEMENTS

14

7. REFERENCES

Beam R. M. and Warming R. F. 1976, *J. Comput. Phys* 22 87.

Beam R.M. and Warming R.F. 1978, *AIAA J.* 16 393.

Boris J.P. and Book D.L. 1973, *J. Comput. Phys* 11 38.

Boris J.P. and Book D.L. 1976a, *J. Comput. Phys* 20 397.

Boris J.P. and Book D.L. 1976b, "Solution of Continuity Equations by the Method of Flux-Corrected Transport", **Methods in Computational Physics**, Vol. 16, Academic Press, New York.

Book D.L., Boris J.P. and Hain K. 1975, *J. Comput. Phys* 18 248.

Hayes D.B. 1973, Lecture notes from the course, "Introduction to Stress Wave Phenomena" taught during the spring of 1973 at Sandia Laboratories, Albuquerque.

Lohner R., Morgan K., Periare J. and Vahdati M. 1987, Finite Element Flux-Corrected Transport (FEM-FCT) for the Euler and Navier-Stokes Equations, ICASE Report 87-4.

Peyret R. and Taylor T.D. 1983, "Computational Methods for Fluid Flow", Springer Series in Computational Physics, New York.

Sod G.A. 1978, *J. Comput. Phys* 27, 1.

Steger J.L. and Warming R.F. 1981, *J. Comput. Phys* 40 263.

Takewaki H. and Yabe T. 1987, *J. Comput. Phys* 70 355.

Warming R.F. and Beam R. M. 1978, On the construction and application of implicit factored schemes for conservation laws, Symposium on Computational Fluid Dynamics, New York, April 16-17, 1977, *SIAM-AMS Proc.* 11 85.

Zalesak S.T. 1979, *J. Comput. Phys* 31 335.

Zalesak S.T. 1981, Very high order and psuedospectral flux-corrected transport (FCT) algorithms for conservation laws, Advances in Computer Methods for Partial Differential Equations-IV, (R. Vichnevetsky and R.S. Stepleman, eds.) IMACS, Rutgers University, 126

15

TABLE 1

Exact solution values for the Riemann problem (see Section 3). The shock velocity U is 1.90, see Appendix B. Note that across the contact discontinuity $x = x_3$, $p_3 = p_4$ and $u_3 = u_4$. The initial conditions are $\rho_1 = 10.0$, $\rho_5 = 1.0$, $p_1 = 10.0$, $p_5 = 1.0$, while $\gamma = 1.4$ throughout.
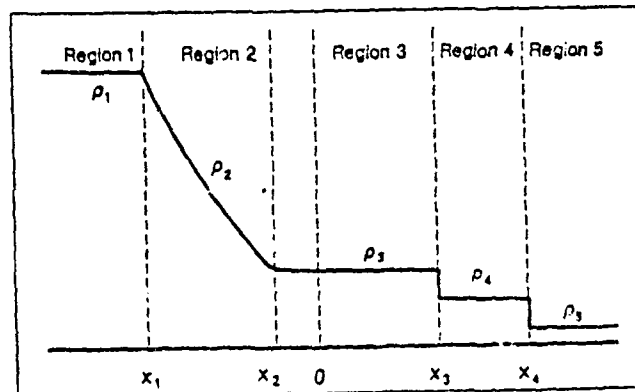
Region i	Density ρ_i	Pressure p_i	Total Energy E_i	Particle Velocity u_i	Boundary x_i
1	10.00	10.00	25.00	0.00	-1.32
2	-	.	.	-	-0.02
3	4.08	2.85	9.05	0.97	-
4	2.04	2.85	8.09	0.97	1.90
5	1.00	1.00	2.50	0.00	-

16

Riemann Problem
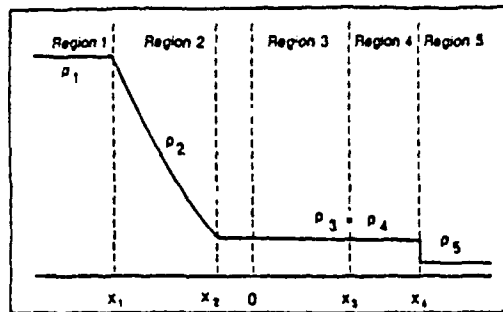

(a) t = 0

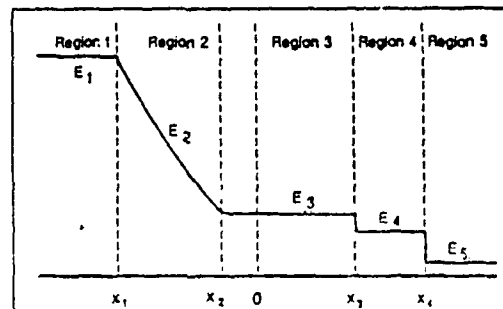Figure 1(a) Initial density profile for the Riemann problem. Diaphragm is at $z = 0$.

(b) t > 0

Figure 1(b) Density profile after the diaphragm has been ruptured. Also is the form of the exact solution, see appendix B.
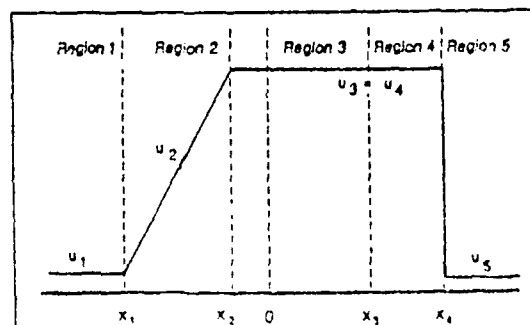
(c) t > 0

Figure 1(c) Same as Fig. 1(b), except pressure profile.

(d) t > 0

Figure 1(d) Same as Fig. 1(b), except total energy per unit volume profile.

(e) t > 0

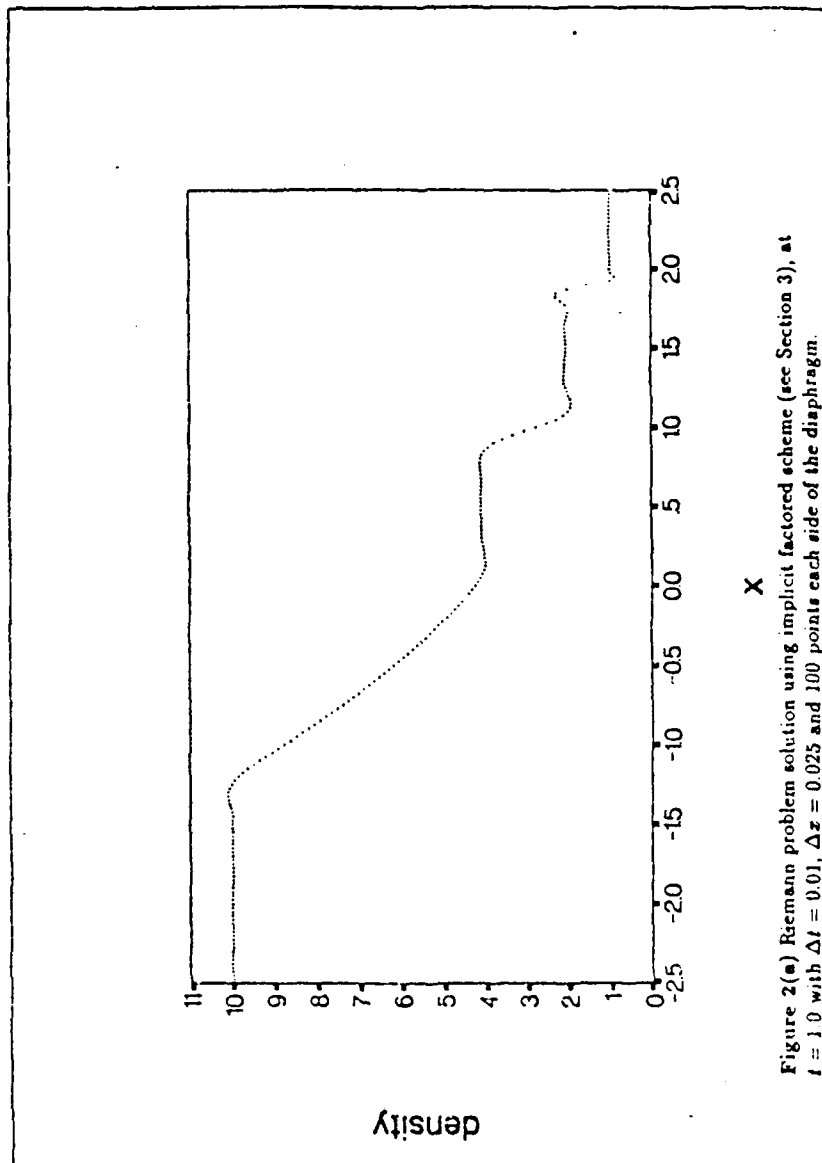Figure 1(e) Same as Fig. 1(c), except particle velocity profile

Figure 2(a) Riemann problem solution using implicit factored scheme (see Section 3), at $t = 1.0$ with $\Delta t = 0.01$, $\Delta z = 0.025$ and 100 points each side of the diaphragm.
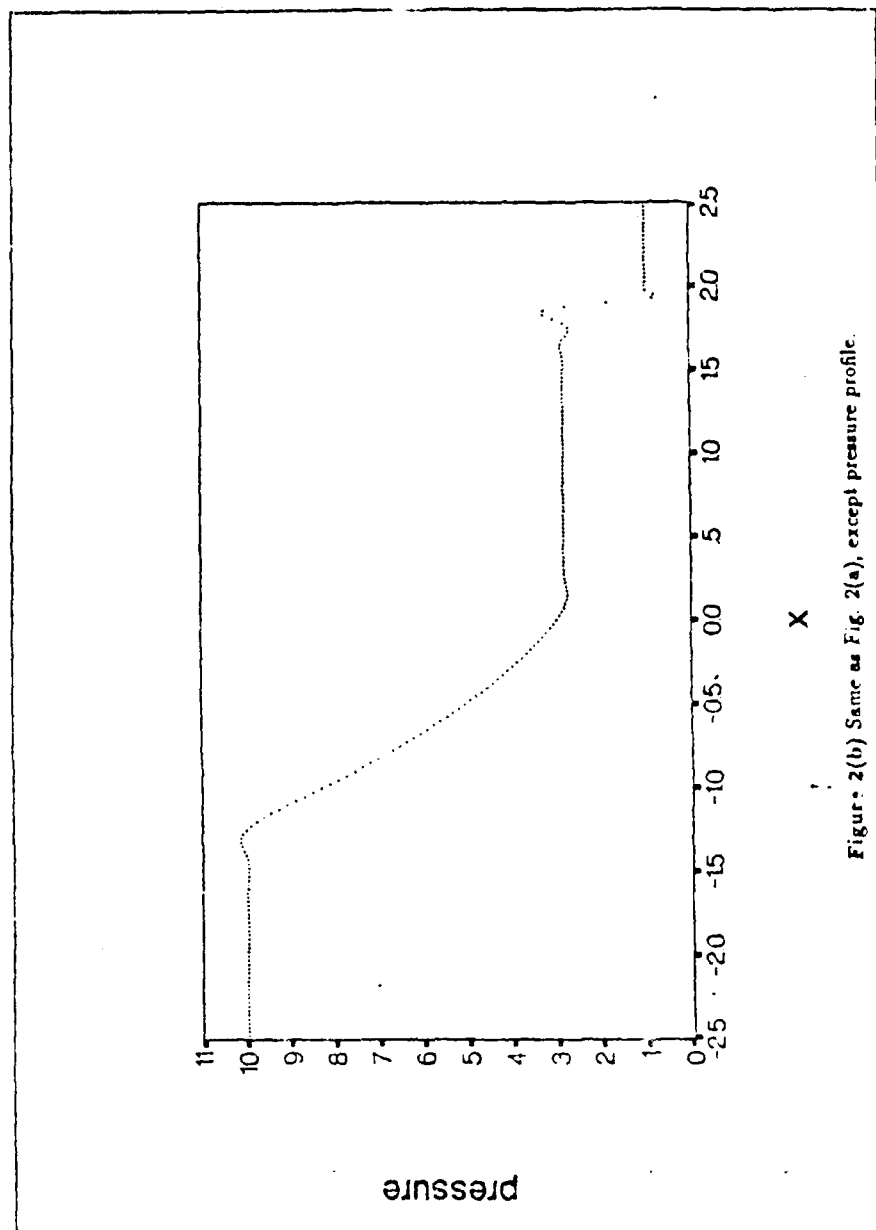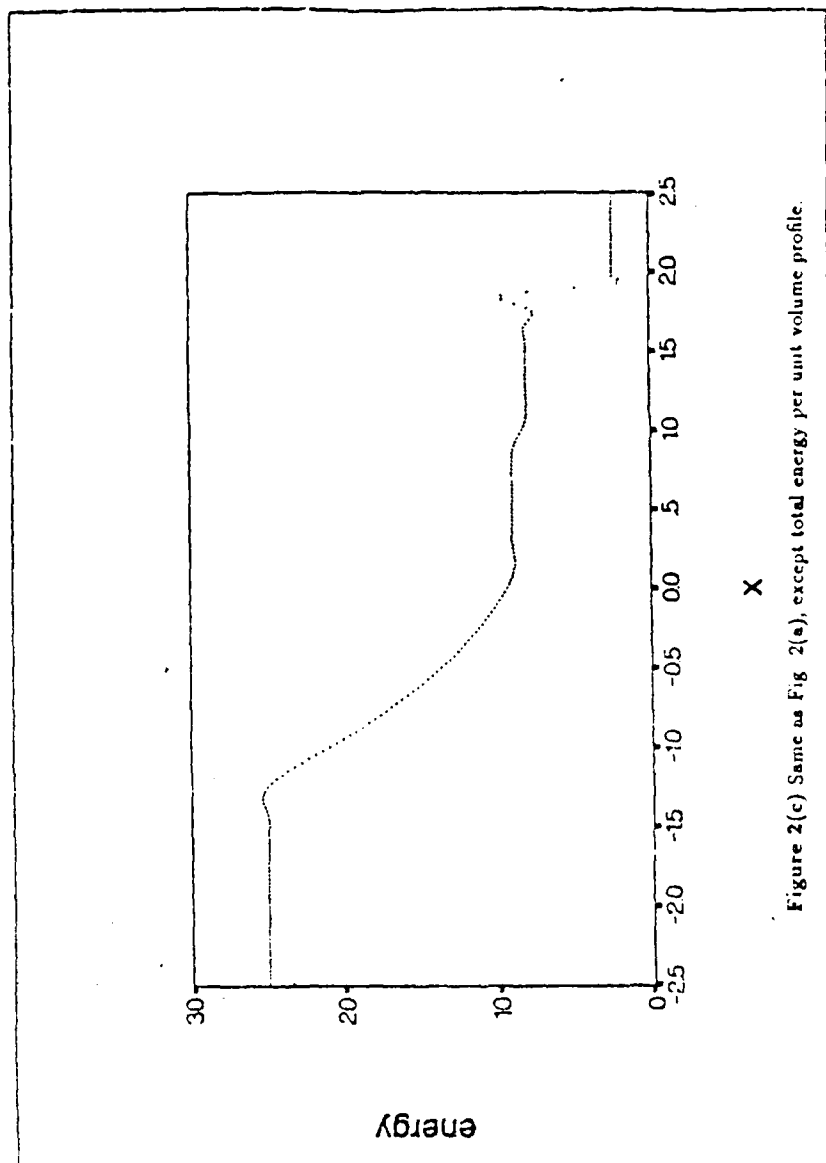
Figure 2(b) Same as Fig. 2(a), except pressure profile.

Figure 2(c) Same as Fig 2(a), except total energy per unit volume profile.
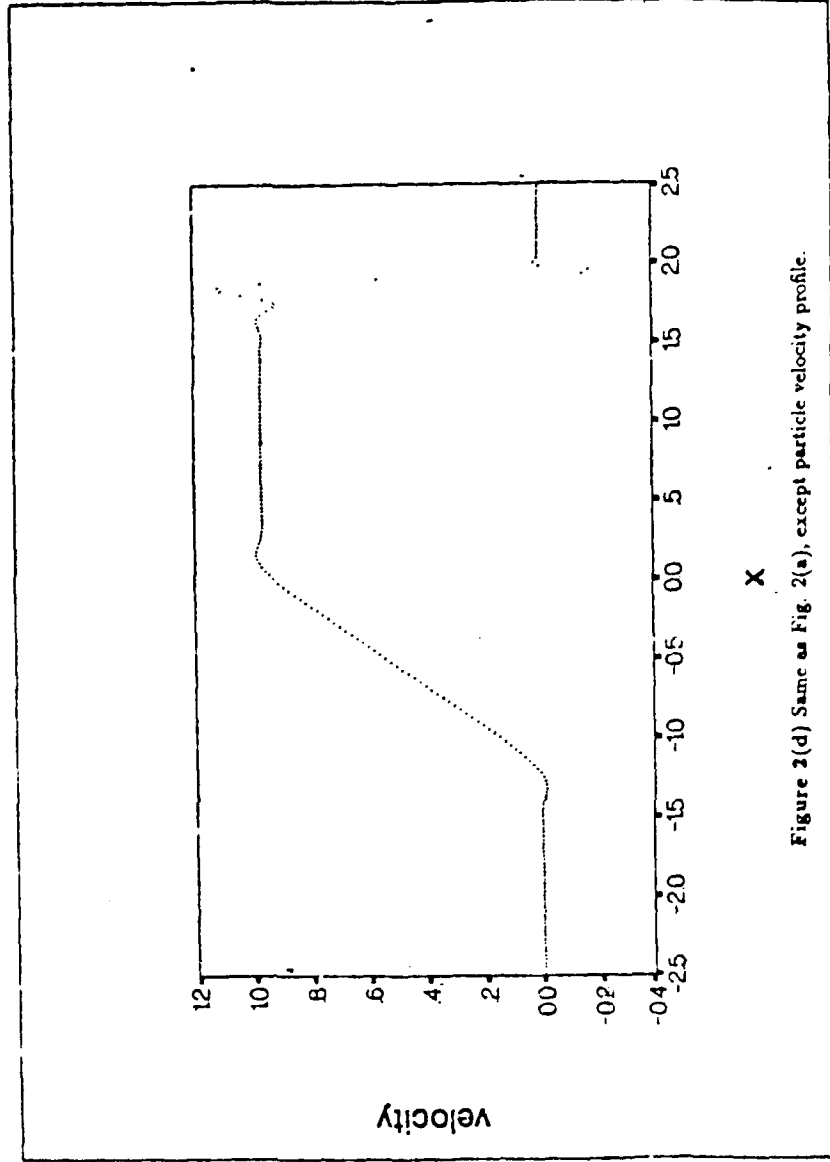
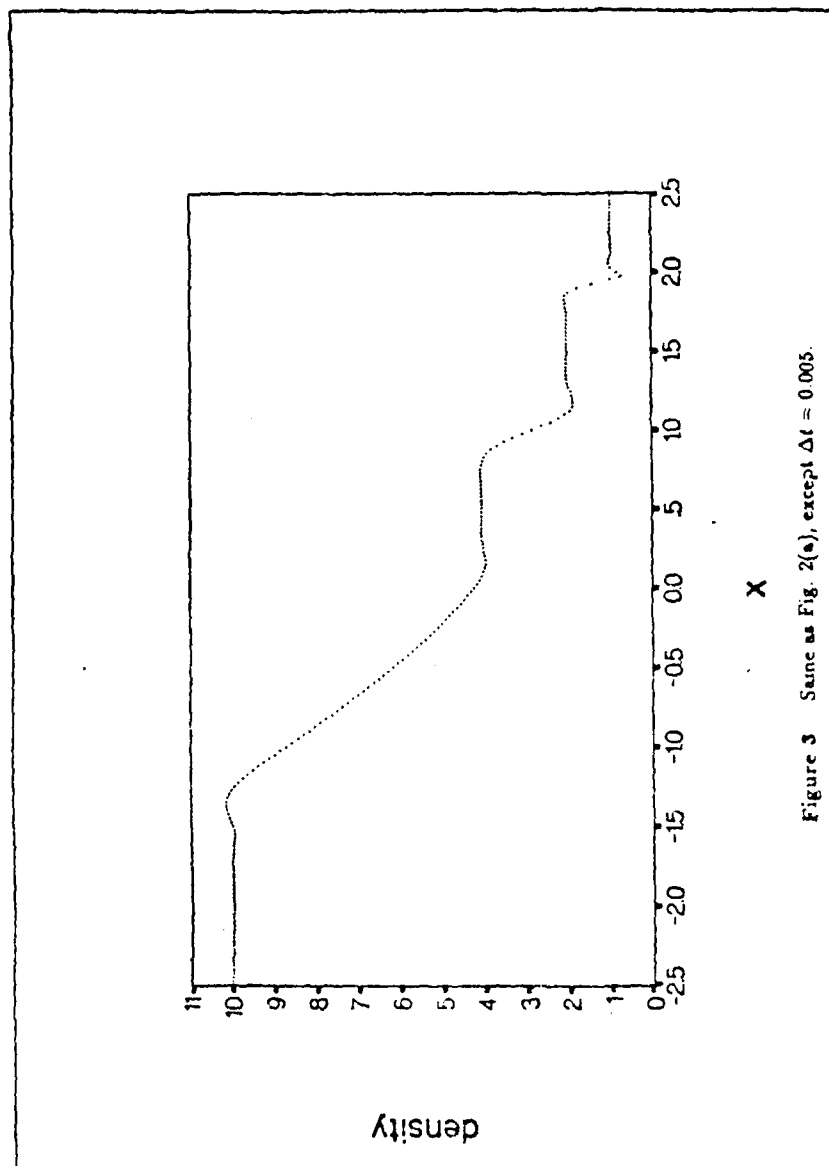Figure 2(d) Same as Fig. 2(a), except particle velocity profile.

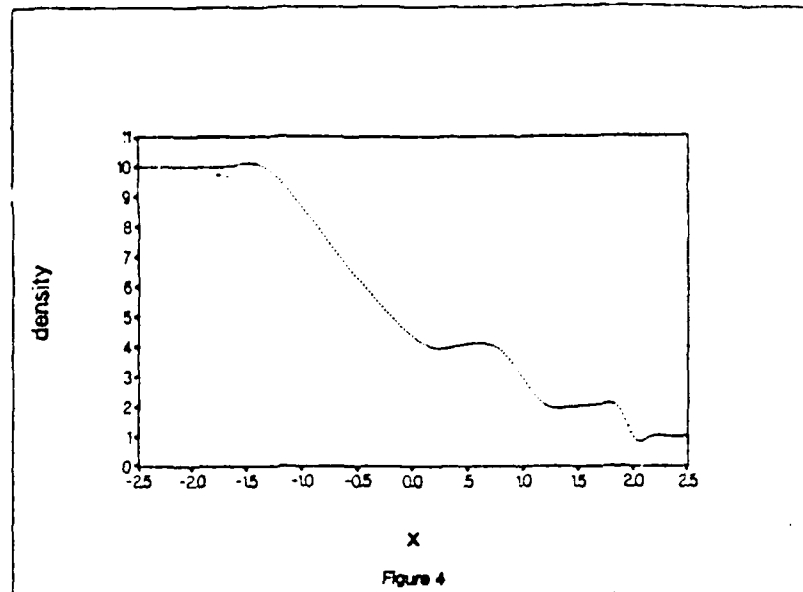Figure 3   Same as Fig. 2(a), except $\Delta t = 0.005$.

Figure 4

Figure 4   Same as Fig. 2(a), except $\Delta t = 0.001$.
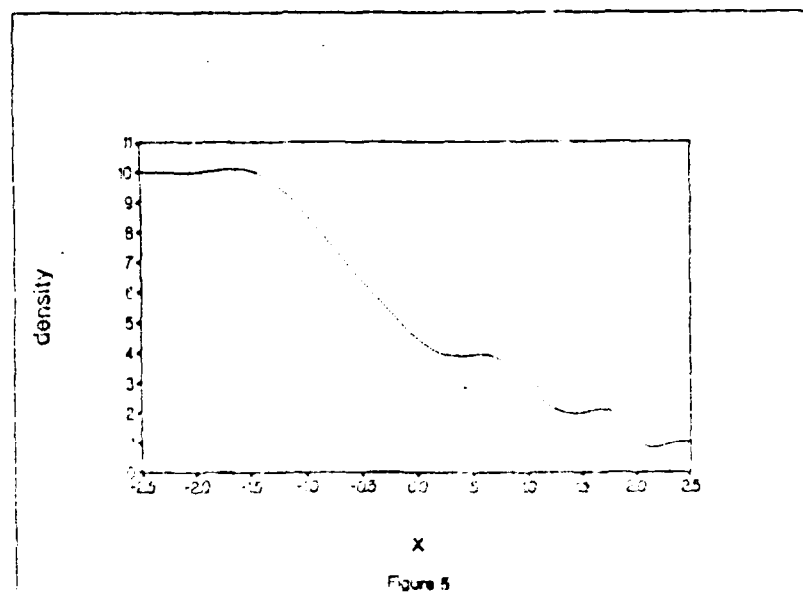

Figure 5

Figure 5   Same as Fig. 2(a), except Δt ·0.001

8. APPENDIX A

In this appendix, the concise form of the implicit factored scheme presented in Section 2 is expanded.

The one-dimensional form of Euler's equations, namely, the continuity equation, conservation of mass and conservation of energy are represented in equations $(A1)$, $(A2)$ and $(A3)$, respectively given by

$$\frac{\partial \rho}{\partial t} + \frac{\partial}{\partial x}(\rho u) = 0 \tag{A1}$$

$$\rho\left(\frac{\partial u}{\partial t} + u\frac{\partial u}{\partial x}\right) + \frac{\partial p}{\partial x} = 0 \tag{A2}$$

$$\rho\left(\frac{\partial \epsilon}{\partial t} + u\frac{\partial \epsilon}{\partial x}\right) + \frac{\partial}{\partial x}(pu) = 0 \tag{A3}$$

where ϵ is the internal energy per unit mass, $p = (\gamma - 1)\rho\epsilon$ from the ideal gas equation of state and γ the ratio of specific heats.

These equations can be written in vector form as

$$\frac{\partial U}{\partial t} + \frac{\partial F(U)}{\partial x} = 0 \tag{A4}$$

where

$$U = \begin{pmatrix} \rho \\ \rho u \\ E \end{pmatrix}, \qquad F(U) = \begin{pmatrix} \rho u \\ \rho u^2 + p \\ (E + p)u \end{pmatrix}$$

and E is the total energy per unit volume and $p = (\gamma - 1)[E - \frac{1}{2}\rho u^2]$

The Eulerian equations of gasdynamics have the property that the nonlinear function $F(U)$ is a homogenous function of degree one in U, see Beam and Warming 1976

Therefore,

$$F(U) = A(U)U \tag{A5}$$

where

$$A(U) = \frac{\partial F}{\partial U} \tag{A6}$$

A-1

is the Jacobian matrix. Hence equation $(A4)$ can be written as

$$\frac{\partial U}{\partial t} + A(U)\frac{\partial U}{\partial x} = 0. \tag{A7}$$

As noted in Section 2 there are numerous examples of implicit time differencing. A single-step temporal scheme for advancing the solution of equation $(A4)$ (Beam and Warming 1978) is

$$U^{n+1} = U^n + \frac{\theta \Delta t}{1+\xi}\left[\left(\frac{\partial U}{\partial t}\right)^n + \left(\frac{\partial U}{\partial t}\right)^{n+1}\right] + \frac{\Delta t}{1+\xi}\left(\frac{\partial U}{\partial t}\right)^n +$$
$$\frac{\xi}{1+\xi}(U^n - U^{n-1}) + O[(\theta - \tfrac{1}{2} - \xi)\Delta t^2 + \Delta t^3]. \tag{A8}$$

Here $U(t) = U(n\Delta t) = U^n$ and Δt is the discrete time increment. θ and ξ define the particular time-difference approximation (see Section 2). Substituting equation $(A4)$ into $(A8)$ gives

$$U^{n+1} = U^n - \frac{\theta \Delta t}{1+\xi}\left[\left(\frac{\partial F}{\partial x}\right)^n + \left(\frac{\partial F}{\partial x}\right)^{n+1}\right] - \frac{\Delta t}{1+\xi}\left(\frac{\partial F}{\partial x}\right)^n +$$
$$\frac{\xi}{1+\xi}(U^n - U^{n-1}) + O[(\theta - \tfrac{1}{2} - \xi)\Delta t^2 + \Delta t^3]. \tag{A9}$$

This equation is nonlinear due to the term involving $F^{n+1} = F(U^{n+1})$. In order to solve for U^{n+1} in equation $(A9)$ the nonlinearity must be removed. A local Taylor expansion about U^n gives

$$F^{n+1} = F^n + \left(\frac{\partial F}{\partial U}\right)^n (U^{n+1} - U^n) + O(\Delta t^2) \tag{A10}$$

substituting in equation $(A6)$

$$F^{n+1} = F^n + A^n(U^{n+1} - U^n) + O(\Delta t^2) \tag{A11}$$

Hence,

$$F^{n+1} = A^n U^{n+1} + O(\Delta t^2) \tag{A12}$$

Therefore, equation $(A9)$ becomes

$$U^{n+1} = U^n - \frac{\theta \Delta t}{1+\xi}\left[\left(\frac{\partial}{\partial x}A^n U^n\right) + \left(\frac{\partial}{\partial x}A^n U^{n+1}\right)\right] - \frac{\Delta t}{1+\xi}\left(\frac{\partial F}{\partial x}\right)^n +$$
$$\frac{\xi}{1+\xi}(U^n - U^{n-1}) + O[(\theta - \tfrac{1}{2} - \xi)\Delta t^2 + \Delta t^3] \tag{A13}$$

A-2

Rearranging equation (A13) gives

$$\left[I + \frac{\theta \Delta t}{1+\xi} \frac{\partial}{\partial x} A^n\right] \Delta U^n = -\frac{\Delta t}{1+\xi}\left(\frac{\partial F}{\partial x}\right)^n + \frac{\xi}{1+\xi}\Delta U^{n-1} \tag{A14}$$

where

$$\Delta U^n = U^{n+1} - U^n. \tag{A15}$$

This equation is a noniterative, second-order time-accurate solution for equation (A4).

The Jacobian matrix A can be simply calculated to be

$$A = \begin{pmatrix} 0 & 1 & 0 \\ (\gamma - 3)\frac{u^2}{2} & (3-\gamma)u & \gamma - 1 \\ (\gamma-1)u^3 - \frac{u\gamma E}{\rho} & \frac{\gamma E}{\rho} - \frac{3}{2}(\gamma-1)u^2 & \gamma u \end{pmatrix} \tag{A16}$$

The eigenvalues of A are

$$\lambda_1 = u, \qquad \lambda_2 = u + c, \qquad \lambda_3 = u - c \tag{A17}$$

where $c = \left(\frac{\gamma p}{\rho}\right)^{\frac{1}{2}}$ is the local speed of sound.

Since F is a homogeneous function (see equation (A5) and Steger and Warming 1981), F can be split into two parts

$$F = F^+ + F^- \tag{A18}$$

where F^+ corresponds to the positive eigenvalues of A and F^- the negative eigenvalues of A.

Any eigenvalue λ_l can be expressed as

$$\lambda_l = \lambda_l^+ + \lambda_l^- \tag{A19}$$

where

$$\lambda_l^+ = \frac{\lambda_l + |\lambda_l|}{2}, \qquad \lambda_l^- = \frac{\lambda_l - |\lambda_l|}{2} \tag{A20}$$

so if $\lambda_l \geq 0$, then $\lambda_l^+ \geq 0$, $\lambda_l^- = 0$ and if $\lambda_l < 0$ then $\lambda_l^- = 0$, $\lambda_l^+ = 0$.

For the system described by (A8) to be hyperbolic there must exist a similarity transformation such that

$$Q^{-1}AQ = \Lambda = \begin{pmatrix} \lambda_1 & & & 0 \\ & \lambda_2 & & \\ & & \ddots & \\ 0 & & & \lambda_m \end{pmatrix} \tag{A21}$$

where Λ is a diagonal matrix and the eigenvalues of A are real.

Hence the diagonal matrix Λ can be expressed as

$$\Lambda = \Lambda^+ + \Lambda^- \tag{A22}$$

where Λ^+ and Λ^- have diagonal elements λ_i^+ and λ_i^-, respectively.

Therefore,

$$A^+ = Q\Lambda^+Q^{-1} \qquad A^- = Q\Lambda^-Q^{-1} \tag{A23}$$

$$\mathbf{F}^+ = A^+U \qquad \mathbf{F}^- = A^-U \tag{A24}$$

and

$$A = A^+ + A^-. \tag{A25}$$

If $\frac{\partial}{\partial x}$ is replaced by the backward difference operator

$$\nabla_x = \mathbf{U}_j - \mathbf{U}_{j-1} \tag{A26}$$

then $(A8)$ is stable if and only if the eigenvalues of A are all positive.

Similarly, if $\frac{\partial}{\partial x}$ is replaced by the forward difference operator

$$\Delta_x = \mathbf{U}_{j+1} - \mathbf{U}_j \tag{A27}$$

then $(A8)$ is stable if and only if the eigenvalues of A are all negative.

A noniterative implicit finite-difference scheme (Beam and Warming 1976), for a one-dimensional system of conservation laws, with the use of split flux vectors $(A23)$ and one-sided spatial difference approximations is

$$\left(\mathbf{I} + \frac{\theta\Delta t}{1+\xi}\frac{\nabla_x A_j^+|^n}{\Delta x}\right)\left(\mathbf{I} + \frac{\theta\Delta t}{1+\xi}\frac{\Delta_x A_j^-|^n}{\Delta x}\right)\Delta\mathbf{U}_j^n$$
$$= -\left(\frac{\Delta t}{2\Delta x(1+\xi)}\right)\left(\delta_x^b\mathbf{F}_j^+|^n + \delta_x^f\mathbf{F}_j^-|^n\right) + \frac{\xi}{1+\xi}\Delta\mathbf{U}_j^{n-1} \tag{A28}$$

where

$$\delta_x^b\mathbf{F}_j = 3\mathbf{F}_j - 4\mathbf{F}_{j-1} + \mathbf{F}_{j-2}$$

and

$$\delta_x^f\mathbf{F}_j = 3\mathbf{F}_j + 4\mathbf{F}_{j+1} - \mathbf{F}_{j+2}$$

By redefining some of these factors, that is,

$$\alpha_i = \frac{\theta\Delta t}{\Delta x(1+\xi)}$$

$$\alpha_2 = \frac{\Delta t}{2\Delta x(1+\xi)}$$

and

$$\alpha_3 = \frac{\xi}{1+\xi}$$

the scheme ($A28$) can be implemented as

$$\left(I + \alpha_1 \nabla_x A_j^+|^n\right)\Delta U_j^* = -\alpha_2\left(\delta_x^b F_j^+|^n + \delta_x^f F_j^-|^n\right) + \alpha_3 \Delta U_j^{n-1} \qquad (A29a)$$

$$\left(I + \alpha_1 \Delta_x A_j^-|^n\right)\Delta U_j^n = \Delta U_j^* \qquad (A29b)$$

$$U_j^{n+1} = U_j^n + \Delta U_j^n. \qquad (A29c)$$

Further simplifing of ($A29$) gives

$$L_j^+|^n \Delta U_j^* = \alpha_1 A_{j-1}^+|^n \Delta U_{j-1}^* - \alpha_2\left(\delta_x^b F_j^+|^n + \delta_x^f F_j^-|^n\right) + \alpha_3 \Delta U_j^{n-1} \qquad (A30a)$$

$$L_j^-|^n \Delta U_j^n = \Delta U_j^* - \alpha_1 A_{j+1}^-|^n \Delta U_{j+1}^n \qquad (A30b)$$

$$U_j^{n+1} = U_j^n + \Delta U_j^n. \qquad (A30c)$$

where

$$L_j^+|^n = I + \alpha_1 A_j^+|^n \qquad \qquad (A31)$$

and

$$L_j^-|^n = I - \alpha_1 A_j^-|^n \qquad (A32)$$

The scheme described by ($A30$) - ($A32$) was used to solve the one-dimensional problem in Section 3.

A-5

9. APPENDIX B

In this appendix, the exact solution for the problem described in Section 3, also known as the Riemann problem, is derived. The derivation follows that of Takewaki and Yabe 1987, except a relation was obtained to find the shock velocity U instead of the Mach number M. The initial conditions, namely a diaphragm placed at $x = 0$ (between the regions 1 and 5), are shown in Fig 1(a). This profile is modified into that in Fig 1(b), when $t > 0$.

The Rankine-Hugoniot conditions (Hayes 1973) across the shock front $x = x_4$ are

$$\frac{\rho_5}{\rho_4} = 1 - \frac{u_4}{U} \qquad (B1)$$

$$p_4 - p_5 = \rho_5 U u_4 \qquad (B2)$$

and

$$E_4 - E_5 = \frac{1}{2}(p_5 + p_4)(v_5 - v_4) \qquad (B3)$$

where

$$v = \frac{1}{\rho}.$$

For a perfect gas

$$E = \frac{pv}{\gamma - 1},$$

therefore equation $(B3)$ becomes

$$p_4 v_4 - p_5 v_5 = \frac{\gamma - 1}{2}(p_5 + p_4)(v_5 - v_4). \qquad (B4)$$

From equation $(B1)$,

$$u_4 = U\left(1 - \frac{\rho_5}{\rho_4}\right). \qquad (B5)$$

Substituting equation $(B5)$ into $(B2)$ gives

$$p_4 - p_5 = U^2(\rho_4 - \rho_5)\frac{\rho_5}{\rho_4}. \qquad (B6)$$

From equation $(B4)$,

$$\frac{p_4}{p_5} \quad \frac{(\gamma + 1)\rho_4 - (\gamma - 1)\rho_5}{(\gamma + 1)\rho_5 - (\gamma - 1)\rho_4} \qquad (B7)$$

B-1

By substituting this equation into (B6), an expression for ρ_4 in terms of the known quantities in region 5 is obtained,

$$\rho_4 = \frac{\rho_5 U^2(\gamma + 1)}{2\gamma p_5 + \rho_5 U^2(\gamma - 1)}. \tag{B8}$$

Substituting equation (B8) into (B7) gives,

$$p_4 = \frac{2\rho_5 U^2 - (\gamma - 1)p_5}{(\gamma + 1)} \tag{B9}$$

and substituting equation (B8) into (B5) gives,

$$u_4 = \frac{2(\rho_5 U^2 - \gamma p_5)}{\rho_5 U(\gamma + 1)}. \tag{B10}$$

The pressure and the velocity should be continuous at the contact surface $x = x_3$. Hence,

$$u_3 = u_4 \tag{B11}$$

and

$$p_3 = p_4. \tag{B12}$$

The particle velocity u is assumed to be a single-valued function of the density ρ in the adiabatic expansion region (region 2). Therefore equations (1) and (2) reduce to

$$\frac{\partial \rho}{\partial t} + \left[u - \left(\frac{\gamma p}{\rho} \right)^{\frac{1}{2}} \right] \frac{\partial \rho}{\partial x} = 0 \tag{B13}$$

if the function $u(\rho)$ satisfies a relation

$$\frac{du}{d\rho} = -\frac{1}{\rho} \left(\frac{\gamma p}{\rho} \right)^{\frac{1}{2}}. \tag{B14}$$

From equation (B13), the velocities of the rarefaction front $(x = x_1)$ and the boundary at $x = x_2$ are $-(\gamma p_1/\rho_1)^{\frac{1}{2}}$ and $u_3 - (\gamma p_3/\rho_3)^{\frac{1}{2}}$, respectively. Integrating the last equation gives

$$u_3 = \left(\frac{\gamma p_1}{\rho_1} \right)^{\frac{1}{2}} \frac{2}{\gamma - 1} \left[1 - \left(\frac{\rho_3}{\rho_1} \right)^{(\gamma-1)/2} \right]. \tag{B15}$$

Since the adiabatic relation

$$\frac{p_3}{p_1} = \left(\frac{\rho_3}{\rho_1} \right)^\gamma \tag{B16}$$

holds, u_3 is related to p_3 as

$$u_3 = \left(\frac{\gamma p_1}{\rho_1}\right)^{\frac{1}{2}} \frac{2}{(\gamma - 1)}\left[1 - \left(\frac{p_3}{p_1}\right)^{\frac{\gamma-1}{2\gamma}}\right].$$
(B17)

Finally by substituting equations $(B9)$, $(B10)$, $(B11)$ and $(B12)$ into $(B17)$, gives the relation which determines the shock velocity

$$\frac{(\gamma - 1)(\rho_5 U^2 - \gamma p_5)}{\rho_5 U(\gamma + 1)}\left(\frac{\rho_1}{\gamma p_1}\right)^{\frac{1}{2}} = 1 - \left(\frac{2\rho_5 U^2 - (\gamma - 1)p_5}{(\gamma + 1)p_1}\right)^{\frac{\gamma-1}{2\gamma}}.$$
(B18)

When equation $(B18)$ was solved using the same parameters in Fig 5 (Table 1) of Takewaki and Yabe 1987, the shock velocities agreed. The numerical values of the exact solution for the problem in Section 3 are given in Table 1.

ABSTRACT

A detailed derivation and analysis of an implicit factored scheme (Beam and
Warming 1976) is given. A one dimensional shock tube problem is solved numerically using
the factored scheme. The results and exact solution are presented for this problem. An
analysis of the features of the method is made and the limitations of this implicit factored
scheme for more general applications to shock waves in solids are discussed. An
alternative approach which has been developed by Boris and Book (1976) appears to have
wider applicability than the method studied here.